

Temporal and Spatial Dependence of Quantum Entanglement: Quantum “Nonlocality” in EPR from Field Theory Perspective

Shih-Yuin Lin*

Physics Division, National Center for Theoretical Science, P.O. Box 2-131, Hsinchu 30013, Taiwan

B. L. Hu†

*Joint Quantum Institute and Department of Physics,
University of Maryland, College Park, Maryland 20742-4111, USA*

(Dated: December 23, 2008)

We consider the entanglement dynamics between two Unruh-DeWitt detectors at rest separated at a distance d . This simple model when analyzed properly in quantum field theory shows many interesting facets and helps to dispel some misunderstandings of entanglement dynamics. We find that there is spatial dependence of quantum entanglement in the stable regime due to the phase difference of vacuum fluctuations the two detectors experience, together with the interference of the mutual influences from the back-reaction of one detector on the other. When two initially entangled detectors are still outside each other’s lightcone, the proportionality of the degree of entanglement to the spatial separation oscillates in time. When the two detectors begin to have causal contact, an interference pattern of the relative degree of entanglement (compared to those at spatial infinity) develops a parametric dependence on d . The detectors separated at those d with stronger relative degree of entanglement enjoy longer disentanglement times. In the cases with weak coupling and large separation, the detectors always disentangle at late times. For sufficiently small d , the two detectors can have residual entanglement even if they initially were in a separable state.

PACS numbers: 03.65.Ud, 03.65.Yz, 03.67.-a

I. INTRODUCTION

Recently we have studied the disentanglement process between two spatially separated Unruh-DeWitt (UD) detectors (point-like objects with internal degrees of freedom) or atoms, described by harmonic oscillators, moving in a common quantum field: One at rest (Alice), the other uniformly accelerating (Rob) [1]. These two detectors are set to be entangled initially, while the initial state of the field is the Minkowski vacuum. In all cases studied in [1] we obtain finite-time disentanglement (called “sudden death” of quantum entanglement [2]), which are coordinate-dependent while the entanglement between the two detectors at two spacetime points is independent of the choice of time slice connecting these two events. Around the moment of complete disentanglement there may be some short-time revival of entanglement within a few periods of oscillations intrinsic to the detectors. In the strong coupling regime, the strong impact of vacuum fluctuations experienced locally by each detector destroys their entanglement right after the coupling is switched on.

In the above situation we find in [1] the event horizon for the uniformly accelerated detector (Rob) cuts off the higher order corrections of mutual influences, and the asymmetric motions of Alice and Rob obscure the dependence of the entanglement and the spatial separation between them. Thus in this paper, we consider the entanglement between two detectors at rest separated at a distance d . This setup, possibly the simplest one could imagine will serve as a concrete model for us to investigate and explicate many subtle points and some essential misconceptions related to quantum entanglement elicited by the classic paper of Einstein-Podolsky-Rosen (EPR) [3].

A. Entanglement at spacelike separation is not acausal: no quantum “nonlocality”

One such misconception (or misnomer, for those who understands the physics but connive to the use of the terminology) is “quantum nonlocality” used broadly and often too loosely in certain communities. In particular, one often has the conception that entanglement set up between two quantum entities (qubits, for example) is independent of

*Electronic address: sylin@phys.cts.nthu.edu.tw

†Electronic address: blhu@umd.edu

their spatial separation, and can exist beyond the causal domains of each. The first part of this statement, spatial independence, is false, as shown already in two earlier papers of the authors [1, 4]; the second part of this statement, i.e., entanglement exists outside of the lightcone (see, e.g., [5, 6]) is true. This is not new and is well known in the quantum field theory context [7], such as in virtual particle exchange processes. What is unfortunate is that some authors think that something acausal is going on (e.g., “spooky action”), and that led to the broad use of the term “quantum nonlocality”. In reality there is nothing nonlocal going on here (see similar outcry in [8]) – quantum mechanics and quantum field theory are local theories so are physical events in our spacetime causal [18].

B. Issues addressed here

With a careful and thorough analysis of this problem we are able to address the following issues:

1) *Spatial separation between two detectors.* Ficek and Tanas [9] as well as Anastopoulos, Shresta and Hu (ASH) [4] studied the problem of two spatially separated qubits interacting with a common electromagnetic field. The former authors while invoking the Born and Markov approximations find the appearance of dark periods and revivals. ASH treat the non-Markovian behavior without these approximations and find a different behavior at short distances. In particular, for weak coupling, they obtain analytic expressions for the dynamics of entanglement at a range of spatial separation between the two qubits, which cannot be obtained when the Born-Markov approximation is imposed. A model with two detectors at rest in a quantum field at finite temperature in (1+1)-dimensional spacetime has been considered by Shiokawa in [10], where some dependence of the early-time entanglement dynamics on spatial separation can also be observed.

In [1] we did not see any simple proportionality between the *initial* separation of Alice and Rob’s detectors and the degree of entanglement: The larger the separation, the weaker the entanglement at some moments, but stronger at others. We wonder this unclear pattern arises because the spatial separation of the two detectors in [1] changes in time and also in coordinate. In our present problem the spatial separation between the two detectors is well defined and remains constant in Minkowski time, so the dependence of entanglement on the spatial separation should be much clearer and distinctly identifiable.

2) *Stronger mutual influences.* Among the cases we considered in [1], the largest correction from the mutual influences is still under 2% of the total while we have only the first and the second order corrections from the mutual influences. There the difficulty for making progress is due to the complicated multi-dimensional integrations in computing the back-and-forth propagations of the backreactions sourced from the two detectors moving in different ways. Here, for the case with both detectors at rest, the integration is simpler and in some regimes we can include stronger and more higher-order corrections of the mutual influences on the evolution of quantum entanglement.

3) *Creation of entanglement and residual entanglement.* In addition to finite time disentanglement and the revival of quantum entanglement for two detectors initially entangled, which have been observed in [1] for a particular initial state, we expect to see other kinds of entanglement dynamics with various initial states and how it varies with spatial separations. Amongst the most interesting behavior we found the creation of entanglement from an initially separated state [16] and the persistence of residual entanglement at late times for two close-by detectors [15].

C. Summary of our findings

When the mutual influences are sufficiently strong (under strong coupling or small separation), the fluctuations of the detectors with low natural frequency will accumulate, then get unstable and blow up. As the separation approaches a merge distance (quantified later), only for detectors with high enough natural frequencies will the fluctuations not diverge eventually but acting more and more like those in the two harmonic oscillator (2HO) quantum Brownian motion (QBM) models [14, 15] (where the two HOs occupy the same spatial location) with renormalized frequencies.

If the duration of interaction is so short that each detector is still outside the lightcone of the other detector, namely, before the first mutual influence reaches one another, the proportionality of the entanglement to the spatial separation oscillates in time: At some moments the larger the separation the weaker the entanglement, but at other moments, the stronger the entanglement.

When a detector gets inside the lightcone of the other, certain interference pattern develops: At distances where the interference is constructive the disentanglement times are longer than those at other distances. This behavior is more distinct when the mutual influences are negligible.

At late times, under proper conditions, the detectors will be entangled if the separation is sufficiently small, and separable if the separation is greater than a specific finite distance. The late-time behavior of the detectors is governed by vacuum fluctuations of the field and independent of the initial state of the detectors.

Since the vacuum can be seen as the simplest medium that the two detectors immersed in, we expect that the intuitions acquired here will be useful in understanding quantum entanglement in atomic and condensed matter systems (upon replacing the field in vacuum by those in the medium). To this extent our results indicate that the dependence of quantum entanglement on spatial separation of qubits could enter in quantum gate operations (see [4] for comments on possible experimental tests of this effect in cavity ions), circuit layout, as well as having an effect on cluster states instrumental to measurement-based quantum computing.

D. Outline of this paper

This paper is organized as follows. In Sec. II we describe our model and the setup. In Sec. III the evolution of the operators are calculated, then the instability for detectors with low natural frequency is described in Sec. IV. We derive the zeroth order results in Sec. V, and the late-time results in Sec. VI. Examples with different spatial separations of detectors in the weak-coupling limit are given in Sec. VII. We conclude with some discussions in Sec. VIII. A late-time analysis on the mode functions is performed in Appendix A, while an early-time analysis of the entanglement dynamics in the weak-coupling limit is given in Appendix B.

II. THE MODEL

Let us consider the Unruh-DeWitt detector theory in (3+1)-dimensional Minkowski space described by the action [1, 11]

$$S = - \int d^4x \frac{1}{2} \partial_\mu \Phi \partial^\mu \Phi + \sum_{j=A,B} \left\{ \int d\tau_j \frac{1}{2} \left[(\partial_{\tau_j} Q_j)^2 - \Omega_0^2 Q_j^2 \right] + \lambda_0 \int d^4x \Phi(x) \int d\tau_j Q_j(\tau_j) \delta^4(x^\mu - z_j^\mu(\tau_j)) \right\}, \quad (1)$$

where the scalar field Φ is assumed to be massless, and λ_0 is the coupling constant. Q_A and Q_B are the internal degrees of freedom of the two detectors, assumed to be two identical harmonic oscillators with mass $m_0 = 1$, bare natural frequency Ω_0 , and the same local time-resolution so their cutoffs Λ_0 and Λ_1 in two-point functions [11] are the same. The left detector is at rest along the world line $z_A^\mu(t) = (t, -d/2, 0, 0)$ and the right detector is sitting along $z_B^\mu(t) = (t, d/2, 0, 0)$. The proper times for Q_A and Q_B are both the Minkowski time, namely, $\tau_A = \tau_B = t$.

We assume at $t = 0$ the initial state of the combined system is a direct product of the Minkowski vacuum $|0_M\rangle$ for the field Φ and a quantum state $|Q_A, Q_B\rangle$ for the detectors Q_A and Q_B , taken to be a squeezed Gaussian state with minimal uncertainty, represented by the Wigner function of the form

$$\rho(Q_A, P_A, Q_B, P_B) = \frac{1}{\pi^2 \hbar^2} \exp -\frac{1}{2} \left[\frac{\beta^2}{\hbar^2} (Q_A + Q_B)^2 + \frac{1}{\alpha^2} (Q_A - Q_B)^2 + \frac{\alpha^2}{\hbar^2} (P_A - P_B)^2 + \frac{1}{\beta^2} (P_A + P_B)^2 \right]. \quad (2)$$

How the two detectors are initially entangled is determined by properly choosing the parameters α and β in Q_A and Q_B . When $\beta^2 = \hbar^2/\alpha^2$, the Wigner function (2) becomes a product of the Wigner function for Q_A, P_A and the one for Q_B, P_B , thus separable. If one further chooses $\alpha^2 = \hbar/\Omega$, then the Wigner function will be initially in the ground state of the two free detectors.

After $t = 0$ the coupling with the field is turned on and the detectors begin to interact with each other through the field. We study the dynamics of quantum entanglement by examining the behavior of the quantity $\Sigma \equiv \det[\mathbf{V}^{PT} + (i\hbar/2)\mathbf{M}]$: For the detectors in Gaussian state, $\Sigma < 0$ if and only if the detectors are entangled. Here \mathbf{M} is the symplectic matrix, \mathbf{V}^{PT} is the partial transpose of the covariance matrix $\mathbf{V}_{\mu\nu} = \langle \mathcal{R}_\mu, \mathcal{R}_\nu \rangle$ with $\mathcal{R}_\mu = (Q_A(t), P_A(t), Q_B(t), P_B(t))$, $\mu, \nu = 1, 2, 3, 4$ [1, 13]. We also define the uncertainty function

$$\Upsilon(t) \equiv \det \left[\mathbf{V} + i \frac{\hbar}{2} \mathbf{M} \right] \quad (3)$$

so that $\Upsilon \geq 0$ is the uncertainty relation [13]. To obtain the correlators $\langle \mathcal{R}_\mu, \mathcal{R}_\nu \rangle$ we are calculating the evolution of operators \mathcal{R}_μ in the following.

III. EVOLUTION OF OPERATORS

Since the combined system (1) is linear, in the Heisenberg picture [11, 12], the operators evolve as

$$\hat{Q}_i(t) = \sqrt{\frac{\hbar}{2\Omega_r}} \sum_j \left[q_i^{(j)}(t) \hat{a}_j + q_i^{(j)*}(t) \hat{a}_j^\dagger \right] + \int \frac{d^3k}{(2\pi)^3} \sqrt{\frac{\hbar}{2\omega}} \left[q_i^{(+)}(t, \mathbf{k}) \hat{b}_{\mathbf{k}} + q_i^{(-)}(t, \mathbf{k}) \hat{b}_{\mathbf{k}}^\dagger \right], \quad (4)$$

$$\hat{\Phi}(x) = \sqrt{\frac{\hbar}{2\Omega_r}} \sum_j \left[f^{(j)}(x) \hat{a}_j + f^{(j)*}(x) \hat{a}_j^\dagger \right] + \int \frac{d^3k}{(2\pi)^3} \sqrt{\frac{\hbar}{2\omega}} \left[f^{(+)}(x, \mathbf{k}) \hat{b}_{\mathbf{k}} + f^{(-)}(x, \mathbf{k}) \hat{b}_{\mathbf{k}}^\dagger \right], \quad (5)$$

with $i, j = A, B$. $q_i^{(j)}$, $q_i^{(\pm)}$, $f^{(j)}$ and $f^{(\pm)}$ are the (c-number) mode functions, \hat{a}_j and \hat{a}_j^\dagger are the lowering and raising operators for the free detector j , while $\hat{b}_{\mathbf{k}}$ and $\hat{b}_{\mathbf{k}}^\dagger$ are the annihilation and creation operators for the free field. The conjugate momenta are $\hat{P}_j(t) = \partial_t \hat{Q}_j(t)$ and $\hat{\Pi}(x) = \partial_t \hat{\Phi}(x)$. The evolution equations for the mode functions have been given in Eqs.(9)-(12) in Ref. [1] with $z_A(t)$ and $z_B(\tau)$ there replaced by $z_A^\mu(t) = (t, -d/2, 0, 0)$ and $z_B^\mu(t) = (t, d/2, 0, 0)$ here. Since we have assumed that the two detectors have the same frequency cutoffs in their local frames, one can do the same renormalization on frequency and obtain their effective equations of motion under the influence of the quantum field [11]:

$$(\partial_t^2 + 2\gamma\partial_t + \Omega_r^2) q_i^{(j)}(t) = \frac{2\gamma}{d} \theta(t-d) \bar{q}_i^{(j)}(t-d), \quad (6)$$

$$(\partial_t^2 + 2\gamma\partial_t + \Omega_r^2) q_i^{(+)}(t, \mathbf{k}) = \frac{2\gamma}{d} \theta(t-d) \bar{q}_i^{(+)}(t-d, \mathbf{k}) + \lambda_0 f_0^{(+)}(z_i(t), \mathbf{k}), \quad (7)$$

where $\bar{q}_B \equiv q_A$, $\bar{q}_A \equiv q_B$, Ω_r is the renormalized frequency, $\gamma \equiv \lambda_0^2/8\pi$, and $f_0^{(+)}(x, \mathbf{k}) \equiv e^{-i\omega t + i\mathbf{k}\cdot\mathbf{x}}$, with $\omega = |\mathbf{k}|$. Here one can see that q_B and q_A are affecting, and being affected by, each other causally with a retardation time d .

The solutions for $q_i^{(j)}$ and $q_i^{(\pm)}$ satisfying the initial conditions $f^{(+)}(0, \mathbf{x}; \mathbf{k}) = e^{i\mathbf{k}\cdot\mathbf{x}}$, $\partial_t f^{(+)}(0, \mathbf{x}; \mathbf{k}) = -i\omega e^{i\mathbf{k}\cdot\mathbf{x}}$, $q_j^{(j)}(0) = 1$, $\partial_t q_j^{(j)}(0) = -i\Omega_r$, and $f_i^{(j)}(0, \mathbf{x}) = \partial_t f_i^{(j)}(0, \mathbf{x}) = q^{(+)}(0; \mathbf{k}) = \partial_t q^{(+)}(0; \mathbf{k}) = \bar{q}_j^{(j)}(0) = \partial_t \bar{q}_j^{(j)}(0) = 0$ (no summation over j), are

$$q_j^{(+)}(\mathbf{k}; t) = \frac{\sqrt{8\pi\gamma}}{\Omega} \sum_{n=0}^{\infty} \theta(t-nd) \left(\frac{2\gamma}{\Omega d} \right)^n e^{(-1)^n i\mathbf{k}_1 z_j^1} \left\{ (M_1 - M_2)^{n+1} e^{-i\omega(t-nd)} + e^{-\gamma(t-nd)} \sum_{m=0}^n (M_1 - M_2)^{n-m} [M_2 W_m(t-nd) - M_1 W_m^*(t-nd)] \right\}, \quad (8)$$

and

$$q_j^{(j)} = \sum_{n=0}^{\infty} q_{2n}, \quad \bar{q}_j^{(j)} = \sum_{n=0}^{\infty} q_{2n+1} \quad (9)$$

(no summation over j), where $\Omega \equiv \sqrt{\Omega_r^2 - \gamma^2}$, $M_1 \equiv (-\omega - i\gamma + \Omega)^{-1}$, $M_2 \equiv (-\omega - i\gamma - \Omega)^{-1}$, $W_0(t) \equiv e^{i\Omega t}$,

$$W_n(t) \equiv \int_0^t dt_{n-1} \sin \Omega(t - t_{n-1}) \int_0^{t_{n-1}} dt_{n-2} \sin \Omega(t_{n-1} - t_{n-2}) \cdots \int_0^{t_1} dt_0 \sin \Omega(t_1 - t_0) W_0(t_0), \quad (10)$$

for $n \geq 1$, and

$$q_n(t) = \theta(t-nd) \left(\frac{2\gamma}{\Omega d} \right)^n e^{-\gamma(t-nd)} [s_1 W_n(t-nd) + s_2 W_n^*(t-nd)], \quad (11)$$

with $s_1 \equiv [1 - \Omega^{-1}(\Omega_r + i\gamma)]/2$, and $s_2 \equiv [1 + \Omega^{-1}(\Omega_r + i\gamma)]/2$.

Using the mode functions Eqs. (8) and (9) one can calculate the correlators of the detectors for the covariance matrix \mathbf{V} [1], each splitting into two parts ($\langle \dots \rangle_a$ and $\langle \dots \rangle_v$) due to the factorized initial state. Because of symmetry, one has $\langle Q_A^2 \rangle = \langle Q_B^2 \rangle$, $\langle P_A^2 \rangle = \langle P_B^2 \rangle$ and $\langle Q_A, P_B \rangle = \langle Q_B, P_A \rangle$. So only six two-point functions need to be calculated for \mathbf{V} .

Since $q_n \sim [\gamma(t-nd)/\Omega d]^n e^{-\gamma(t-nd)}/n!$ for large t , q_n will reach its maximum amplitude ($\approx (n/e\Omega d)^n/n!$) around $t-nd \approx n/\gamma$, which makes the numerical error of the long-time behavior of \mathbf{V} difficult to control. Fortunately for the late-time behavior for all d and the long-time behavior for very small or very large d , we still have good approximations, as we shall see below. However, before we proceed, the issue of instability should be addressed first.

IV. INSTABILITY OF LOW-FREQUENCY HARMONIC OSCILLATORS

Combining the equations of motion for $q_A^{(A)}$ and $q_B^{(A)}$, one has

$$(\partial_t^2 + 2\gamma\partial_t + \Omega_r^2) q_{\pm}^{(A)}(t) = \pm \frac{2\gamma}{d} q_{\pm}^{(A)}(t-d). \quad (12)$$

where $q_{\pm}^{(A)}(t) \equiv q_A^{(A)}(t) \pm q_B^{(A)}(t)$. For $t > d$ and when d is small, one may expand $q_{\pm}^{(A)}(t-d)$ around t so that

$$(\partial_t^2 + 2\gamma\partial_t + \Omega_r^2) q_{\pm}^{(A)}(t) = \pm \frac{2\gamma}{d} \left[q_{\pm}^{(A)}(t) - d\partial_t q_{\pm}^{(A)}(t) + \frac{d^2}{2} \partial_t^2 q_{\pm}^{(A)}(t) - \frac{d^3}{3!} \partial_t^3 q_{\pm}^{(A)}(t) + \dots \right], \quad (13)$$

or

$$\left[\partial_t^2 + 4\gamma\partial_t + \left(\Omega_r^2 - \frac{2\gamma}{d} \right) \right] q_+^{(A)}(t) = O(\gamma d), \quad (14)$$

$$\left[\partial_t^2 + \left(\Omega_r^2 + \frac{2\gamma}{d} \right) \right] q_-^{(A)}(t) = O(\gamma d). \quad (15)$$

If we start with a small renormalized frequency Ω_r and a small spatial separation $d < 2\gamma/\Omega_r^2$ with γd kept small so the $O(\gamma d)$ terms can be neglected, then $q_+^{(A)}$ will be exponentially growing since its effective frequency becomes imaginary ($\Omega_r^2 - (2\gamma/d) < 0$), while $q_-^{(A)}$ oscillates without damping. Similar argument shows that $q_{\pm}^{(B)}$ will have the same instability when two harmonic oscillators with small Ω_r^2 are situated close enough to each other.

One may wonder whether the $O(\gamma d)$ terms can alter the above observations. In Appendix A we perform a late-time analysis, which shows the same instability. The conclusion is, if $\Omega_r^2 < 2\gamma/d$, all the mode functions will grow exponentially in time so the correlators $\langle Q_i, Q_j \rangle$ or the quantum fluctuations of the detectors diverge at late times. Accordingly, we define

$$d_{ins} \equiv 2\gamma/\Omega_r^2 \quad (16)$$

as the ‘‘radius of instability’’. For two detectors with separation $d > d_{ins}$, the system is stable. For the cases with $d = d_{ins}$, a constant solution for $q_+^{(j)}$ at late times is acquired by (14), while for $d < d_{ins}$, the system is unstable

Below we restrict our discussion to the stable regime, $\Omega_r^2 > 2\gamma/d$.

V. ZEROth ORDER RESULTS

Neglecting the mutual influences, the v-part of the zeroth-order cross correlators read

$$\langle Q_A(t), Q_B(t) \rangle_v^{(0)} = \frac{\hbar}{\pi\Omega^2 d} \text{Re} \frac{i}{\Omega + i\gamma} \left\{ [\Omega + e^{-2\gamma t} (\Omega + 2\gamma e^{i\Omega t} \sin \Omega t)] \mathcal{S}_d - e^{-\gamma t} [(\Omega \cos \Omega t + \gamma \sin \Omega t) (\mathcal{S}_{d-t} + \mathcal{S}_{d+t}) + (\Omega + i\gamma) \sin \Omega t (\mathcal{C}_{d-t} - \mathcal{C}_{d+t})] \right\}, \quad (17)$$

$$\langle P_A(t), P_B(t) \rangle_v^{(0)} = \frac{\hbar}{\pi\Omega^2 d} \text{Re} i(\Omega + i\gamma) \left\{ [\Omega + e^{-2\gamma t} (\Omega - 2\gamma e^{i\Omega t} \sin \Omega t)] \mathcal{S}_d - e^{-\gamma t} [(\Omega \cos \Omega t - \gamma \sin \Omega t) (\mathcal{S}_{d-t} + \mathcal{S}_{d+t}) + (\Omega - i\gamma) \sin \Omega t (\mathcal{C}_{d-t} - \mathcal{C}_{d+t})] \right\}, \quad (18)$$

$$\begin{aligned} \langle P_A(t), Q_B(t) \rangle_v^{(0)} &= \langle Q_A(t), P_B(t) \rangle_v^{(0)} \\ &= \frac{\hbar\gamma}{\pi\Omega^2 d} e^{-\gamma t} \sin \Omega t \text{Re} \left\{ -2e^{(-\gamma+i\Omega)t} \mathcal{S}_d + \mathcal{S}_{d-t} + \mathcal{S}_{d+t} + i(\mathcal{C}_{d-t} - \mathcal{C}_{d+t}) \right\}, \end{aligned} \quad (19)$$

where $\mathcal{S}_x \equiv \frac{1}{2}(\text{Ci}[(\Omega + i\gamma)x] + \text{Ci}[-(\Omega + i\gamma)x]) \sin[(\Omega + i\gamma)x] - \text{Si}[(\Omega + i\gamma)x] \cos[(\Omega + i\gamma)x]$ and $\mathcal{C}_x \equiv \frac{1}{2}(\text{Ci}[(\Omega + i\gamma)x] + \text{Ci}[-(\Omega + i\gamma)x]) \cos[(\Omega + i\gamma)x] + \text{Si}[(\Omega + i\gamma)x] \sin[(\Omega + i\gamma)x]$ with sine integral $\text{Si}(x) = \text{si}(x) + \pi/2$ and cosine integral $\text{Ci}(x)$ [17]. The a-part of the zeroth order correlators as well as the two-point functions (for a single inertial detector), $\langle Q_j^2 \rangle_v^{(0)}$, $\langle Q_j, P_j \rangle_v^{(0)}$, and $\langle P_j^2 \rangle_v^{(0)}$ are all independent of the spatial separation d (for explicit expressions see Eqs. (25) of Ref. [1] and Appendix A of Ref. [12]). So the d -dependence of the zeroth-order degree of entanglement $\Sigma^{(0)}$ are all coming from (17)-(19), which are due to the phase difference of vacuum fluctuations that the detectors experience locally.

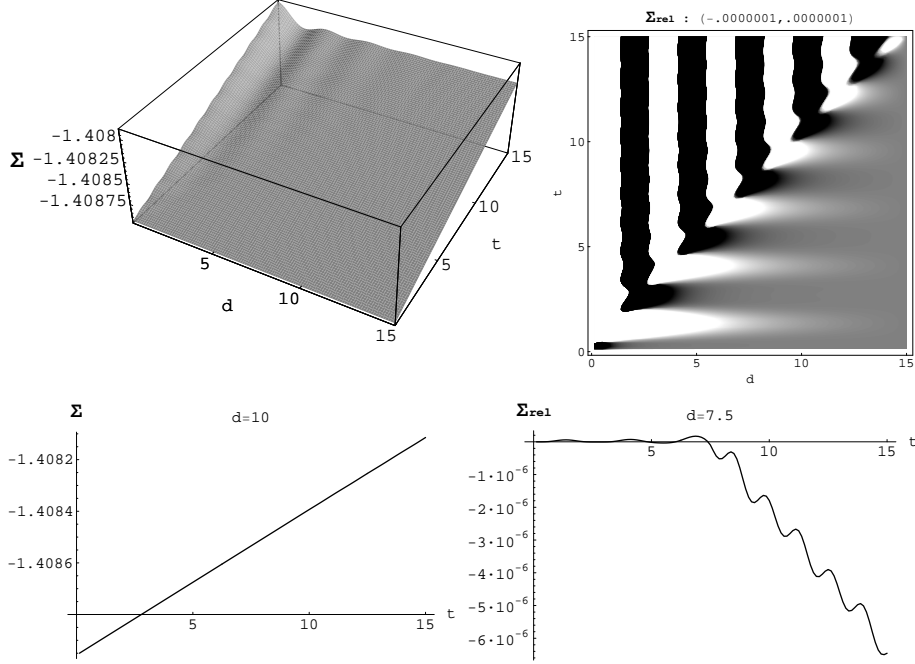


FIG. 1: The zeroth order results, no mutual influence is included here. $\gamma = 10^{-5}$, $\Omega = 2.3$, $\Lambda_0 = \Lambda_1 = 20$, and $(\alpha, \beta) = (1.1, 4.5)$. The two plots on the left are for the zeroth-order $\Sigma^{(0)}$, which is seen to increase and disentangle in time. The two plots on the right are for the relative values of $\Sigma^{(0)}$ at spatial separation d to the value at infinite spatial separation, namely, $\Sigma_{\text{rel}}^{(0)} \equiv \Sigma^{(0)}(d) - \Sigma^{(0)}(\infty)$. In the upper-right plot, the brighter color corresponds to higher value of $\Sigma_{\text{rel}}^{(0)}$.

Note that when

$$d \rightarrow d_{\min} \equiv \frac{1}{\Omega} e^{1-\gamma E - \Lambda_1}, \quad (20)$$

one has $\langle \mathcal{R}_A(t), \mathcal{R}_B(t) \rangle_{\text{v}}^{(0)} \rightarrow \langle \mathcal{R}_A(t)^2 \rangle_{\text{v}}^{(0)} = \langle \mathcal{R}_B(t)^2 \rangle_{\text{v}}^{(0)}$, $\mathcal{R} = P, Q$. That is, the two detectors should be seen as located at the same spatial point when $d \approx d_{\min}$ in our model, which is actually a coarse-grained effective theory. Let us call d_{\min} the “merge distance”.

A. Early-time entanglement dynamics inside the lightcone ($d < t$)

In the weak-coupling limit ($\gamma\Lambda_1 \ll \Omega$), when the separation d is not too small, the effect from the mutual influences comes weakly and slowly, so the zeroth order correlators dominate the early-time behavior of the detectors. The asymptotic expansions of sine-integral and cosine-integral functions read [17]

$$\text{Ci}[(\Omega + i\gamma)x] \approx \frac{i\pi}{2} \left(\frac{x}{|x|} - 1 \right) + \frac{\sin(\Omega + i\gamma)x}{(\Omega + i\gamma)x}, \quad (21)$$

$$\text{Si}[(\Omega + i\gamma)x] \approx \frac{\pi}{2} \frac{x}{|x|} - \frac{\cos(\Omega + i\gamma)x}{(\Omega + i\gamma)x}, \quad (22)$$

for $\Omega > 0$ and $\gamma > 0$ and $|(\Omega + i\gamma)x| \gg 1$. So in the weak-coupling limit, from $t - d = 0$ up to $t - d \sim O(1/\gamma)$, one has

$$\langle Q_A(t), Q_B(t) \rangle_{\text{v}}^{(0)} \approx \theta(t - d) \frac{\sin \Omega d}{\Omega d} \frac{\hbar}{2\Omega} e^{-\gamma d} \left[1 - e^{-2\gamma(t-d)} \right], \quad (23)$$

$\langle P_A(t), P_B(t) \rangle_{\text{v}}^{(0)} \approx \Omega^2 \langle Q_A(t), Q_B(t) \rangle_{\text{v}}^{(0)}$ and $\langle P_A(t), Q_B(t) \rangle_{\text{v}}^{(0)}, \langle Q_A(t), P_B(t) \rangle_{\text{v}}^{(0)} \sim O(\gamma/\Omega)$. The $\theta(t-d)$ implies the onset of a clear interference pattern ($\sim \sin \Omega d / \Omega d$) inside the lightcone, as shown in Fig. 1. This is mainly due to the sign flipping of the sine integral function Si_{d-t} in (17)-(19) around $d = t$ when $d - t$ changes sign. The $\theta(t-d)$

acts like that each detector starts to “know” the existence of the other detector when they enter the lightcone of each other, though the mutual influences are not considered here. In the next subsection we will see that there exists some interference pattern of $O(\gamma)$ in Σ even for $d > t$, where no classical signal can reach one detector from the other.

B. Outside the lightcone ($d > t$)

Before the first mutual influences from one detector reaches the other, the zeroth order results are exact. From (21) and (22), when $d \gg t$, one has

$$\langle Q_A(t), Q_B(t) \rangle_v^{(0)} \approx \frac{2\gamma}{\pi\Omega^4 d^2} \left[1 + e^{-2\gamma t} \left(\cos \Omega t + \frac{\gamma}{\Omega} \sin \Omega t \right)^2 - \frac{2d^2 e^{-\gamma t}}{d^2 - t^2} \left(\cos \Omega t + \frac{\gamma}{\Omega} \sin \Omega t \right) \right], \quad (24)$$

$$\langle P_A(t), P_B(t) \rangle_v^{(0)} \approx \frac{2\gamma}{\pi d^2} e^{-2\gamma t} \frac{\sin^2 \Omega t}{\Omega^2}, \quad (25)$$

$$\langle P_A(t), Q_B(t) \rangle_v^{(0)} = \langle Q_A(t), P_B(t) \rangle_v^{(0)} \approx \frac{2\gamma e^{-\gamma t} \sin \Omega t}{\pi\Omega^2 d^2} \frac{1}{\Omega} \left[-e^{-\gamma t} \left(\cos \Omega t + \frac{\gamma}{\Omega} \sin \Omega t \right) + \frac{d^2}{d^2 - t^2} \right], \quad (26)$$

which makes the value of Σ depend on d and t , that is, the dependence of the degree of entanglement on the spatial separation d between the two detectors varies in time t .

In the weak-coupling limit, with the initial state (2), one has, to $O(\gamma/\Omega)$,

$$\begin{aligned} \Sigma^{(0)}(d) - \Sigma^{(0)}(\infty)|_{d \gg t} &\approx \frac{\gamma \hbar (\hbar^2 - \alpha^2 \beta^2)}{4\alpha^2 \beta^2 \pi \Omega^4 d^2} \left\{ \hbar (\alpha^2 \Omega^2 - \beta^2) e^{-4\gamma t} \left(1 + e^{-2\gamma t} - \frac{2d^2}{d^2 - t^2} e^{-\gamma t} \cos \Omega t \right) \right. \\ &\left. - e^{-2\gamma t} [\hbar (\alpha^2 \Omega^2 + \beta^2) - (e^{-2\gamma t} - e^{-4\gamma t}) (\hbar - \alpha^2 \Omega) (\beta^2 - \hbar \Omega)] \left(\cos 2\Omega t + e^{-2\gamma t} - \frac{2d^2}{d^2 - t^2} e^{-\gamma t} \cos \Omega t \right) \right\}, \quad (27) \end{aligned}$$

so at large times, the relative value of Σ at $d \gg t$ compared to the value when the detectors are separated at infinite distance is given approximately by

$$\Sigma_{\text{rel}}^{(0)}(d) \equiv \Sigma^{(0)}(d) - \Sigma^{(0)}(\infty) \approx \frac{\gamma \hbar^2 (\alpha^2 \beta^2 - \hbar^2)}{4\alpha^2 \beta^2 \pi \Omega^4 d^2} (\alpha^2 \Omega^2 + \beta^2) e^{-2\gamma t} \cos 2\Omega t, \quad (28)$$

which oscillates in frequency 2Ω for $\alpha^2 \beta^2 \neq \hbar^2$, though the magnitude is small and decays in time. This explains the pattern outside the lightcone in the upper-right plot and the small oscillations before $t \approx 7.5$ in the lower-right plot of Fig. 1. We conclude that, before one detector enters the lightcone of the other, at some moments the larger the separation, the weaker the entanglement, but at other moments, the stronger the entanglement.

C. Breakdown of the zeroth order results

At late times $t \gg \gamma^{-1}$, all $\langle \dots \rangle_a$ vanish, so $\langle \dots \rangle_v$ dominate and the nonvanishing two-point correlation functions read

$$\langle Q_A, Q_B \rangle^{(0)}|_{t \gg \gamma^{-1}} \approx \frac{\hbar}{\pi \Omega d} \text{Re} \frac{i \mathcal{S}_d}{\Omega + i \gamma}, \quad (29)$$

$$\langle P_A, P_B \rangle^{(0)}|_{t \gg \gamma^{-1}} \approx \frac{\hbar}{\pi \Omega d} \text{Re}(i\Omega - \gamma) \mathcal{S}_d, \quad (30)$$

$$\langle Q_A^2 \rangle^{(0)}|_{t \gg \gamma^{-1}} = \langle Q_B^2 \rangle^{(0)}|_{t \gg \gamma^{-1}} \approx \frac{i\hbar}{2\pi\Omega} \ln \frac{\gamma - i\Omega}{\gamma + i\Omega}, \quad (31)$$

$$\langle P_A^2 \rangle^{(0)}|_{t \gg \gamma^{-1}} = \langle P_B^2 \rangle^{(0)}|_{t \gg \gamma^{-1}} \approx \frac{\hbar}{\pi} \left\{ \frac{i}{2\Omega} (\Omega^2 - \gamma^2) \ln \frac{\gamma - i\Omega}{\gamma + i\Omega} + \gamma \left[2\Lambda_1 - \ln \left(1 + \frac{\gamma^2}{\Omega^2} \right) \right] \right\}, \quad (32)$$

from (17)-(19) and from Ref. [12].

When $d \rightarrow \infty$, the cross correlators vanish and the uncertainty relation reads

$$\Upsilon^{(0)}|_{t \gg \gamma^{-1}} \equiv \det \left[\mathbf{V}^{(0)}|_{t \gg \gamma^{-1}} + \frac{i}{2} \hbar \mathbf{M} \right] \approx \left(\langle Q_A^2 \rangle^{(0)} \langle P_A^2 \rangle^{(0)}|_{t \gg \gamma^{-1}} - \frac{\hbar^2}{4} \right)^2 \geq 0, \quad (33)$$

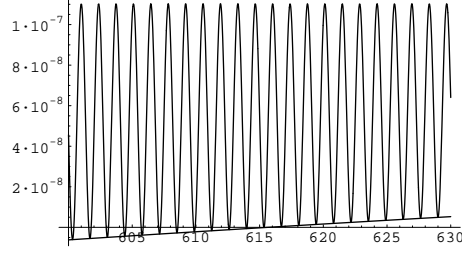


FIG. 2: The oscillating curve represents the value of $\Upsilon^{(0)}$ (defined in (33)) as a function of d . The bottom curve represents its lower bound (Eq.(34)). It becomes negative when $d < 616$, which signifies the violation of uncertainty relation. To rectify this, one needs to add on the mutual influences, as shown in Fig. 3. Here $\gamma = 10^{-4}$, $\Omega = 2.3$, $\Lambda_0 = \Lambda_1 = 25$.

for sufficiently large Λ_1 [12], so the uncertainty relation holds perfectly. However, observing that $|\mathcal{S}_d| \approx \pi e^{-\gamma d}$ for d large enough but still finite, the late-time $\Upsilon^{(0)}$ can reach the lowest values

$$\begin{aligned} & \left(\langle Q_A^2(t) \rangle^{(0)} \langle P_A^2(t) \rangle^{(0)} |_{t \gg \gamma^{-1}} - \frac{\hbar^2}{4} \right)^2 + \frac{\hbar^4 e^{-4\gamma d}}{16\Omega_r^4 d^4} - \\ & \frac{\hbar^2 e^{-2\gamma d}}{4d^2} \left[\frac{\hbar^2}{2\Omega_r^2} + \left(\langle Q_A^2(t) \rangle^{(0)} |_{t \gg \gamma^{-1}} \right)^2 + \Omega_r^{-4} \left(\langle P_A^2(t) \rangle^{(0)} |_{t \gg \gamma^{-1}} \right)^2 \right]. \end{aligned} \quad (34)$$

This zeroth order result suggests that the uncertainty relation can fail if d is not large enough to make the value of the second line of (34) overwhelmed by the first line. When this happens the zeroth-order results break down. Therefore to describe the long-time entanglement dynamics at short distances d the higher order corrections from the mutual influences must be included for consistency.

When $\gamma \ll \gamma\Lambda_1 \ll \Omega$, one has a simple estimate that the late time $\Upsilon^{(0)}$ becomes negative if d is smaller than about $d_0 \approx \pi/2\Lambda_1\gamma$, which is much greater than d_{ins} found in Sec.IV.

VI. ENTANGLEMENT AT LATE TIMES

Since all $q_i^{(j)}$ vanish at late times in the stable regime (see Appendix A), the late-time correlators consist of $q_j^{(\pm)}$ only, for example,

$$\langle Q_B^2 \rangle |_{t \rightarrow \infty} = \int \frac{\hbar d^3 k}{(2\pi)^3 2\omega} q_B^{(+)}(t, \mathbf{k}) q_B^{(-)}(t, \mathbf{k}) |_{t \rightarrow \infty}, \quad (35)$$

where $q_B^{(+)}(t, \mathbf{k}) |_{t \rightarrow \infty}$ is given by (A12) and $q_B^{(-)}(t, \mathbf{k}) |_{t \rightarrow \infty}$ is its complex conjugate. After some algebra, we find that the value of correlators at late times can be written as

$$\langle Q_A^2 \rangle |_{t \rightarrow \infty} = \langle Q_B^2 \rangle |_{t \rightarrow \infty} = 2\text{Re}(\mathcal{F}_{0+} + \mathcal{F}_{0-}), \quad (36)$$

$$\langle Q_A, Q_B \rangle |_{t \rightarrow \infty} = 2\text{Re}(\mathcal{F}_{0+} - \mathcal{F}_{0-}), \quad (37)$$

$$\langle P_A^2 \rangle |_{t \rightarrow \infty} = \langle P_B^2 \rangle |_{t \rightarrow \infty} = 2\text{Re}(\mathcal{F}_{2+} + \mathcal{F}_{2-}), \quad (38)$$

$$\langle P_A, P_B \rangle |_{t \rightarrow \infty} = 2\text{Re}(\mathcal{F}_{2+} - \mathcal{F}_{2-}), \quad (39)$$

where

$$\mathcal{F}_{c\pm}(\gamma, \Omega, d) \equiv \frac{\hbar i}{4\pi} \int_0^{\omega_{max}} \frac{\omega^c}{\omega^2 + 2i\gamma\omega - \Omega^2 \pm \frac{2\gamma}{d} e^{i\omega d}}, \quad (40)$$

and ω_{max} is the high frequency (UV) cutoff corresponding to Λ_1 .

In the stable regime one can write $\mathcal{F}_{c\pm}$ in a series form:

$$\begin{aligned} \mathcal{F}_{c\pm}(\gamma, \Omega, d) &= \frac{\hbar i}{4\pi} \int_0^{\omega_{max}} d\omega \frac{\omega^c}{\omega^2 + 2i\gamma\omega - \Omega^2 - \gamma^2} \sum_{n=0}^{\infty} \left[\frac{\mp \frac{2\gamma}{d} e^{i\omega d}}{\omega^2 + 2i\gamma\omega - \Omega^2 - \gamma^2} \right]^n \\ &= \frac{\hbar i}{4\pi} \int_0^{\omega_{max}} d\omega \sum_{n=0}^{\infty} \frac{1}{n!} \left[\mp \frac{\gamma}{\Omega d} e^{i\omega d} \partial_{\Omega} \right]^n \frac{\omega^c}{\omega^2 + 2i\gamma\omega - \Omega^2 - \gamma^2}, \end{aligned} \quad (41)$$

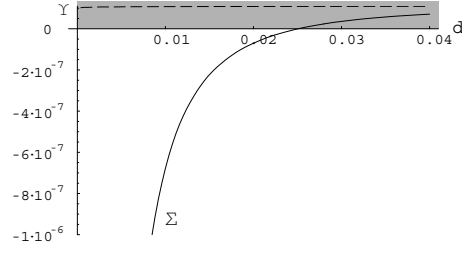


FIG. 3: Plots for Σ (solid curve) and Υ (dashed curve) at late times as a function of d , with parameters the same as those in Fig. 2. Two detectors are separable when $\Sigma \geq 0$ (shaded zone). One can see that Σ becomes negative when $d < 0.025$. With the mutual influences included, the uncertainty relation (see Eq.(3) and below) now holds for all d .

so we have

$$\mathcal{F}_{0\pm}(\gamma, \Omega, d) = \frac{\hbar}{4\pi} \left\{ \frac{i}{2\Omega} \ln \frac{\gamma - i\Omega}{\gamma + i\Omega} + \sum_{n=1}^{\infty} \frac{1}{n!} \left[\mp \frac{\gamma}{\Omega d} \partial_{\Omega} \right]^n \operatorname{Re} \frac{i}{\Omega} e^{(\gamma+i\Omega)nd} \Gamma[0, (\gamma+i\Omega)nd] \right\}, \quad (42)$$

$$\begin{aligned} \mathcal{F}_{2\pm}(\gamma, \Omega, d) = & \frac{\hbar}{4\pi} \left\{ \frac{i}{2\Omega} (\Omega^2 - \gamma^2) \ln \frac{\gamma - i\Omega}{\gamma + i\Omega} + \gamma \left[2\Lambda_1 - \ln \left(1 + \frac{\gamma^2}{\Omega^2} \right) \right] + \right. \\ & \left. \sum_{n=1}^{\infty} \frac{1}{n!} \left[\mp \frac{\gamma}{\Omega d} \partial_{\Omega} \right]^n \operatorname{Re} \frac{i}{\Omega} e^{(\gamma+i\Omega)nd} (\gamma + i\Omega)^2 \Gamma[0, (\gamma + i\Omega)nd] \right\}, \end{aligned} \quad (43)$$

for large frequency cutoff ω_{max} , or the corresponding Λ_1 .

Substituting the late-time correlators (36)-(39) into the covariance matrix \mathbf{V} [1], we get

$$\Sigma|_{t \rightarrow \infty} = \left(16\operatorname{Re}\mathcal{F}_{0+}\operatorname{Re}\mathcal{F}_{2-} - \frac{\hbar^2}{4} \right) \left(16\operatorname{Re}\mathcal{F}_{0-}\operatorname{Re}\mathcal{F}_{2+} - \frac{\hbar^2}{4} \right), \quad (44)$$

$$\Upsilon|_{t \rightarrow \infty} = \left(16\operatorname{Re}\mathcal{F}_{0+}\operatorname{Re}\mathcal{F}_{2+} - \frac{\hbar^2}{4} \right) \left(16\operatorname{Re}\mathcal{F}_{0-}\operatorname{Re}\mathcal{F}_{2-} - \frac{\hbar^2}{4} \right). \quad (45)$$

Numerically we found that $16\operatorname{Re}\mathcal{F}_{0-}\operatorname{Re}\mathcal{F}_{2+} - (\hbar^2/4)$ and $\Upsilon|_{t \rightarrow \infty}$ are positive definite in the cases considered in this paper, so if $16\operatorname{Re}\mathcal{F}_{0+}\operatorname{Re}\mathcal{F}_{2-} - (\hbar^2/4)$ is negative, then $\Sigma < 0$, and the detectors are entangled.

In the weak-coupling limit, keeping the correlators to $O(\gamma/d)$, we have

$$16\operatorname{Re}\mathcal{F}_{0+}\operatorname{Re}\mathcal{F}_{2-} - \frac{\hbar^2}{4} \approx \frac{\hbar^2\gamma\Lambda_1}{\pi\Omega} - \frac{\hbar^2}{\Omega^3} \operatorname{Re} \left\{ \left[\frac{i\gamma\Omega}{\pi d} + \frac{2\gamma^2\Lambda_1}{\pi^2 d} (i + \Omega d) \right] e^{i\Omega d} \Gamma[0, i\Omega d] \right\}, \quad (46)$$

which is positive as $d \rightarrow \infty$, but negative when $d \rightarrow 0_+$. So (46) must cross zero at a finite “entanglement distance” $d_{ent} > 0$ where $\Sigma = 0$. For $d < d_{ent}$, the detectors will have residual entanglement, while for $d > d_{ent}$, the detectors are separable at late times.

For small γ , d_{ent} is almost independent of γ . We find that when $\Lambda \sim O(10)$, $\Omega \sim O(1)$,

$$d_{ent} \approx \frac{1/\Omega}{\frac{\pi}{2} + \frac{\Lambda_1}{\pi/2}}. \quad (47)$$

is a good estimate. Here d_{ent} is still much larger than the “merge distance” d_{min} in (20). For example, as shown in Fig. 3, when $\gamma = 0.0001$, $\Omega = 2.3$, $\Lambda_1 = 25$, one has $d_{ent} \approx 0.025$, which is quite a bit greater than the “radius of instability” $2\gamma/\Omega^2 \approx 3.8 \times 10^{-5}$, and much greater than the merge distance $d_{min} \approx 9 \times 10^{-12}$.

A corollary follows. If the initial state of the two detectors with $d < d_{ent}$ is separable, then the residual entanglement implies that there is an entanglement creation during the evolution. In contrast, if the initial state of the two detectors with $d > d_{ent}$ is entangled, then the late-time separability implies that they disentangled in a finite time. Examples will be given in the next section.

Note that the ill behavior of $\Upsilon^{(0)}$ has been cured by mutual influences. The uncertainty function (45) is positive for all d at late times.

Note also that, while the corrections from the mutual influences to $\langle Q_A^2 \rangle|_{t \rightarrow \infty}$ and $\langle P_A^2 \rangle|_{t \rightarrow \infty}$ are $O(\gamma/d)$, the mutual influences have been included in the leading order approximation for the cross correlators. Indeed, in (41), even as low as $n = 1$, we have had

$$\langle Q_A, Q_B \rangle|_{t \rightarrow \infty} \approx \langle Q_A, Q_B \rangle^{(0)}|_{t \rightarrow \infty} - \frac{2\hbar\gamma}{\pi} \frac{4\gamma}{d} \int_0^\infty d\omega \frac{\omega [(\Omega_r^2 - \omega^2) \cos \omega d - 2\gamma\omega \sin \omega d]}{[(\omega^2 - \Omega_r^2)^2 + 4\gamma^2\omega^2]^2}. \quad (48)$$

However, this is slightly different from the approximation with the first order mutual influences included. Writing the $n = 0$ and $n = 1$ terms in Eq. (8) as

$$q_j^{(+)} \approx q_{j,n=0}^{(+)} + q_{j,n=1}^{(+)}, \quad (49)$$

then the approximated cross correlator with the first order mutual influences included is the ω integration of $\text{Re} [(q_{A,n=0}^{(+)} + q_{A,n=1}^{(+)})(q_{B,n=0}^{(+)} + q_{B,n=1}^{(+)})]$, but in (48) only $\text{Re} [q_{A,n=0}^{(+)}q_{B,n=0}^{(+)} + q_{A,n=0}^{(+)}q_{B,n=1}^{(+)} + q_{A,n=1}^{(+)}q_{B,n=0}^{(+)}]$ contribute, though there are $O(\gamma^0)$ terms in $q_{A,n=1}^{(+)}q_{B,n=1}^{(+)}$. The latter is small for $\Omega d \gg 1$, and will be canceled by the mutual influences of higher orders.

VII. ENTANGLEMENT DYNAMICS IN WEAK-COUPPLING LIMIT

A. Disentanglement at very large distance

Suppose the two detectors are separated far enough ($d \gg \Omega$) so that the cross correlations and the mutual influences can be safely ignored. Then in the weak-coupling limit ($\Omega \gg \gamma\Lambda_1$) the zeroth order results for the v-part of the self correlators dominate, so that [1],

$$\langle Q_A^2 \rangle_v = \langle Q_B^2 \rangle_v \approx \frac{\hbar}{2\Omega} (1 - e^{-2\gamma t}), \quad (50)$$

$$\langle P_A^2 \rangle_v = \langle P_B^2 \rangle_v \approx \frac{\hbar}{2}\Omega (1 - e^{-2\gamma t}) + \frac{2}{\pi}\hbar\gamma\Lambda_1, \quad (51)$$

and $\langle Q_A, P_A \rangle_v = \langle Q_B, P_B \rangle_v \sim O(\gamma)$, while the v-part of the cross correlators are vanishingly small. This is exactly the case we have considered in Sec. IV.A.2 of Ref. [1], where we found

$$\Sigma \approx \frac{\hbar^2 e^{-4\gamma t}}{16\alpha^2\beta^2\Omega^2} [Z_8 (e^{-4\gamma t} - 2e^{-2\gamma t}) + Z_4] + \frac{\hbar^3\gamma\Lambda_1}{4\pi\alpha^2\beta^2\Omega^2} Z_2 e^{-2\gamma t} + \frac{\hbar^4}{\pi^2\Omega^2} \gamma^2 \Lambda_1^2, \quad (52)$$

with $Z_8 \geq 0$, $Z_8 - Z_4 \geq 0$ and $Z_2 \geq 0$ (Z_8 , Z_4 and Z_2 are parameters depending on α and β , defined in Eqs.(37), (38) and (41) of Ref. [1], respectively.) Accordingly the detectors always disentangle in a finite time. There are two kinds of behaviors that Σ could have. For $Z_4 > 0$, the disentanglement time is a function of Z_4 , Z_8 and γ ,

$$t_{dE>}^{(0)} \approx -\frac{1}{2\gamma} \ln \left(1 - \sqrt{1 - \frac{Z_4}{Z_8}} \right), \quad (53)$$

while for $Z_4 < 0$, the disentanglement time is much longer,

$$t_{dE<}^{(0)} \approx \frac{1}{2\gamma} \ln \frac{|Z_4|\pi/(2\hbar\gamma\Lambda_1)}{Z_2 + \sqrt{Z_2^2 - 4\alpha^2\beta^2 Z_4}}, \quad (54)$$

and depends on Λ_1 .

B. Disentanglement at long distance

When d is large (so $1/\Omega d$ is small) but not too large to make all the mutual influences negligible, while the zeroth order results for the v-part of the self correlators (50) and (51) are still good, the first order correction ($n = 1$ terms

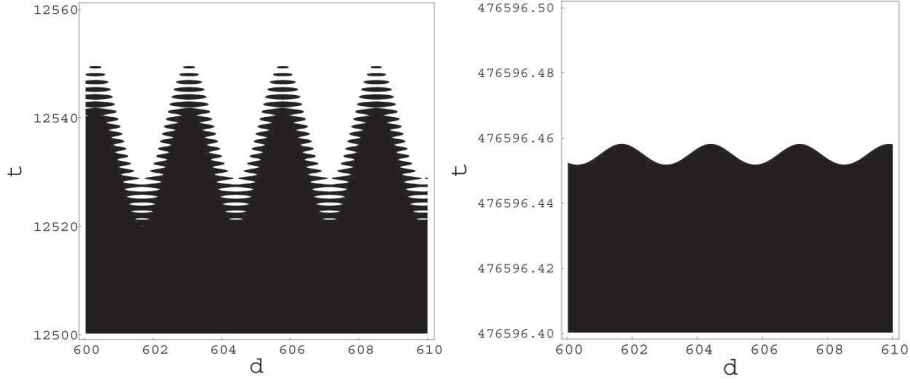


FIG. 4: The plot of Σ as a function of d and t . Σ is negative in the dark region and positive in the bright region. For a fixed d , the disentanglement time t_{dE} is at the border of the lowest dark region, or the earliest time that becoming separable. The interference pattern in Fig. 1 for Σ at early times signifies that the disentanglement time t_{dE} longer or shorter than those at $d \rightarrow \infty$ (Eqs. (53) and (54)). The grided profile in the left plot shows that after t_{dE} there could be some short-time revivals of entanglement. Here the parameters are the same as those in Fig. 1 except $(\alpha, \beta) = (1.5, 0.2)$ in the left plot and $(1.1, 4.5)$ in the right (cf. Fig. 3 in Ref. [1].)

in (8)) to the cross correlators $\langle Q_A, Q_B \rangle$ can be of the same order of $\langle Q_A, Q_B \rangle^{(0)}$ (a similar observation on the late-time correlators has been mentioned in the end of Sec. VI.) Including the first order correction, for $d > O(1/\sqrt{\gamma\Omega})$, we have a simple expression,

$$\begin{aligned} \langle Q_A, Q_B \rangle_v &= \langle Q_A, Q_B \rangle_v^{(0)} + \theta(t-d) \frac{\hbar \sin \Omega d}{2\Omega} \frac{e^{-\gamma d}}{\Omega d} \left[-1 + e^{-2\gamma(t-d)} (1 + 2(t-d)\gamma) + O(\gamma/\Omega) \right] \\ &\approx \theta(t-d) \frac{\hbar \sin \Omega d}{\Omega} \frac{e^{-\gamma d}}{\Omega d} \gamma (t-d) e^{-2\gamma(t-d)}, \end{aligned} \quad (55)$$

and $\langle P_A, P_B \rangle_v \approx \Omega^2 \langle Q_A, Q_B \rangle_v$ with other two-point functions $\langle \dots \rangle_v$ being $O(\gamma)$ for all t . Here $\langle Q_A, Q_B \rangle_v^{(0)}$ in the weak-coupling limit has been shown in (23). The above approximation is good over the time interval from $t = 0$ up to $e^{-2\gamma(t-d)} > O(\gamma/\Omega)$, namely, before $t-d \sim O(-\gamma^{-1} \ln(\gamma/\Omega))$.

Still, in this first order approximation, $\langle Q_A, Q_B \rangle_v$ and $\langle P_A, P_B \rangle_v$ are the only correlators depending on the separation d . Inserting those approximated expressions for the correlators into the definition of Σ [1], we find that the interference pattern in d for the relative values of Σ at early times (Fig. 1) can last through the disentanglement process to make the disentanglement time t_{dE} longer or shorter than those at $d \rightarrow \infty$, though the contrast decays noticeably compared with those at early times. Two examples are shown in Fig. 4. For $Z_4 > 0$, the disentanglement time is about

$$t_{dE>} \approx t_{dE>}^{(0)} - \frac{Z_6 \left(t_{dE>}^{(0)} - d \right) e^{\gamma d} \sin \Omega d}{Z_8 d \left(1 - e^{-2\gamma t_{dE>}^{(0)}} \right) + Z_6 \left[1 - 2\gamma \left(t_{dE>}^{(0)} - d \right) \right] e^{\gamma d} \sin \Omega d}, \quad (56)$$

where $Z_6 \equiv (\hbar^2 - \alpha^2 \beta^2)(\alpha^2 \Omega^2 - \beta^2)$ (Fig. 4 (left).) For $Z_4 < 0$, the correction of $\sin \Omega d$ is below the precision of $t_{dE<}^{(0)}$ estimated in (54). Here we just show the numerical result (up to the first order mutual influences, which is still a good approximation around the disentanglement time in that case) in Fig. 4 (right), which shows that the interference pattern in d are suppressed but still nonvanishing for large disentanglement times.

C. Entanglement generation at very short distance

When $\Omega d \sim O(\epsilon)$, $\gamma/\Omega \sim O(\epsilon^2)$, and $\epsilon \ll 1$, one can perform a dimensional reduction on the third derivatives in (13), namely,

$$\ddot{q}_{\pm}^{(j)} \approx -\frac{\Omega_r^2 \mp \frac{2\gamma}{d}}{1 \mp \gamma d} \dot{q}_{\pm}^{(j)}, \quad (57)$$

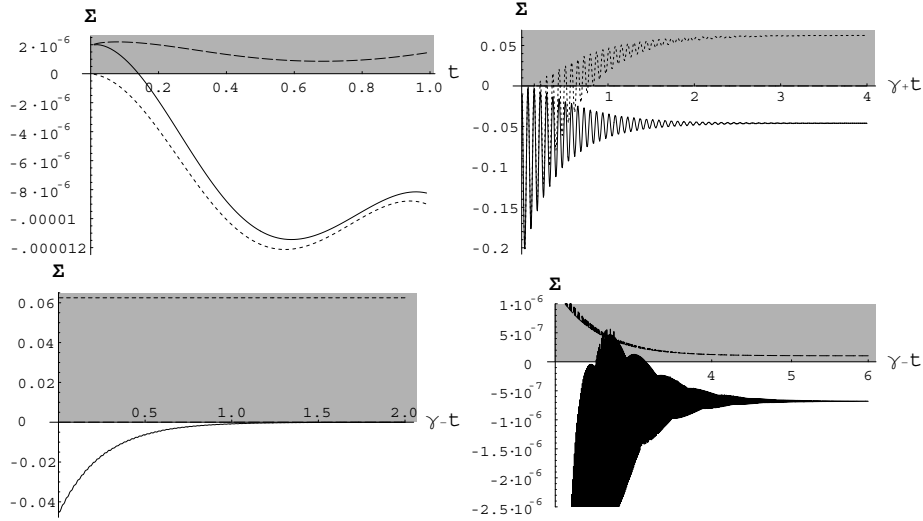


FIG. 5: (Upper-left) The solid curve and the long-dashed curve represent the values of Σ and Υ , respectively, while the dotted line is for the value of Σ with all $\langle \dots \rangle_v$ set to zero. The detectors are separable initially (the parameters here are the same as those in Figs. 2 and 3 except $d = 0.01$ and $(\alpha, \beta) = (1, 1)$.) Quantum entanglement has been generated after $t \approx 0.15$, and Σ oscillates in frequency Ω_+ at early times. Around the time scale $t \sim 1/\gamma_+$ (≈ 5000 here) (upper-right), Σ has an oscillation with long period $\pi/(\Omega_- - \Omega_+)$ (≈ 361.4). Σ appears to be settling down at a value (about -0.046 here) depending in this case only on the value α in the initial data. However, in a much longer time scale $t \sim 1/\gamma_-$ ($\approx 1.13 \times 10^8$) (lower-left), one sees that the value of $|\Sigma|$ is actually decaying exponentially to the late-time value ($\approx -6.8 \times 10^{-7}$) consistent with the results in Fig. 3 with $d = 0.01$ and independent of the initial data of the detectors.

to obtain, up to $O(\epsilon^5)$,

$$\ddot{q}_{\pm}^{(j)} + 2\gamma_{\pm}\dot{q}_{\pm}^{(j)} + \Omega_{\pm}^2 q_{\pm}^{(j)} \approx 0, \quad (58)$$

$$\ddot{q}_{\pm}^{(+)} + 2\gamma_{\pm}\dot{q}_{\pm}^{(+)} + \Omega_{\pm}^2 q_{\pm}^{(+)} \approx \lambda_{\pm} \left(e^{-ik_1 d/2} \pm e^{ik_1 d/2} \right) e^{-i\omega t}, \quad (59)$$

where $j = A, B$, $q_{\pm}^{(+)} \equiv q_A^{(+)} \pm q_B^{(+)}$ and

$$\gamma_- \equiv \frac{\gamma d^2 (\Omega_r^2 + \frac{2\gamma}{d})}{6 (1 + \gamma d)^2}, \quad (60)$$

$$\gamma_+ \equiv \frac{2\gamma}{1 - \gamma d} - \frac{\gamma d^2 (\Omega_r^2 - \frac{2\gamma}{d})}{6 (1 - \gamma d)^2}, \quad (61)$$

$$\Omega_{\pm}^2 \equiv \frac{\Omega_r^2 \mp \frac{2\gamma}{d}}{1 \mp \gamma d}, \quad \lambda_{\pm} \equiv \frac{\lambda_0}{1 \mp \gamma d}. \quad (62)$$

Here γ_-/γ_+ is of $O(\epsilon^2)$. Note that q_-^j and the decay modes in $q_-^{(+)}$ have sub-radiant behavior, while q_+^j and the decay modes in $q_+^{(+)}$ are super-radiant. For small d , the time scale $\gamma_-^{-1} \gg \gamma^{-1} > \gamma_+^{-1} \approx 1/2\gamma$, and γ_-^{-1} goes to infinity as $d \rightarrow 0$.

The solutions for (58) and (59) with suitable initial conditions are

$$q_j^{(j)} \pm \bar{q}_j^{(j)} = \frac{1}{2} e^{-\gamma_{\pm} t} [s_1^{\pm} e^{i\Omega_{\pm} t} + s_2^{\pm} e^{-i\Omega_{\pm} t}], \quad (63)$$

$$q_A^{(+)} \pm q_B^{(+)} = \frac{\lambda_{\pm}}{\Omega_{\pm}} \left(e^{-ik_1 d/2} \pm e^{ik_1 d/2} \right) [(M_1^{\pm} - M_2^{\pm}) e^{-i\omega t} + e^{-\gamma_{\pm} t} (M_2^{\pm} e^{i\Omega_{\pm} t} - M_1^{\pm} e^{-i\Omega_{\pm} t})], \quad (64)$$

where $s_1^{\pm} \equiv [1 - \Omega_{\pm}^{-1}(\Omega_r + i\gamma_{\pm})]/2$, $s_2^{\pm} \equiv [1 + \Omega_{\pm}^{-1}(\Omega_r + i\gamma_{\pm})]/2$, $M_1^{\pm} \equiv (-\omega - i\gamma_{\pm} + \Omega_{\pm})^{-1}$, and $M_2^{\pm} \equiv (-\omega - i\gamma_{\pm} - \Omega_{\pm})^{-1}$. Actually these solutions are the zeroth order results with γ and Ω replaced by γ_{\pm} and Ω_{\pm} . So we can easily reach the simple expressions

$$\langle Q_A^2 \rangle_v \approx \frac{\lambda_+^2}{16\pi\gamma_+} \left[\langle Q_A^2 \rangle_v^{(0)} + \langle Q_A, Q_B \rangle_v^{(0)} \right]_{\gamma \rightarrow \gamma_+}^{\Omega \rightarrow \Omega_+} + \frac{\lambda_-^2}{16\pi\gamma_-} \left[\langle Q_A^2 \rangle_v^{(0)} - \langle Q_A, Q_B \rangle_v^{(0)} \right]_{\gamma \rightarrow \gamma_-}^{\Omega \rightarrow \Omega_-}, \quad (65)$$

$$\langle Q_A, Q_B \rangle_v \approx \frac{\lambda_+^2}{16\pi\gamma_+} \left[\langle Q_A, Q_B \rangle_v^{(0)} + \langle Q_A^2 \rangle_v^{(0)} \right]_{\gamma \rightarrow \gamma_+}^{\Omega \rightarrow \Omega_+} + \frac{\lambda_-^2}{16\pi\gamma_-} \left[\langle Q_A, Q_B \rangle_v^{(0)} - \langle Q_A^2 \rangle_v^{(0)} \right]_{\gamma \rightarrow \gamma_-}^{\Omega \rightarrow \Omega_-}, \quad (66)$$

and so on. Here $\langle \dots \rangle_v^{(0)}$ are those expressions given in (17)-(19) above and in Eqs.(A9) and (A10) of Ref.[12] ($\langle Q_A, P_A \rangle_v = \partial_t \langle Q_A^2 \rangle_v / 2$.) The pre-factors $\lambda_{\pm}^2 / 16\pi\gamma_{\pm}$ are put there because in our definitions for the zeroth order results the overall factor λ_0^2 has been expressed in terms of $8\pi\gamma$, but now $\gamma_{\pm} \neq \lambda_{\pm} / 8\pi$.

In Fig. 5 we demonstrate an example in which the two detectors are separable in the beginning but get entangled at late times. There are three stages in their history of evolution:

1. At a very early time ($t \approx 0.15$) quantum entanglement has been generated. This entanglement generation is dominated by the mutual influences sourced by the initial information in the detectors and mediated by the field. (For more early-time analysis, see Appendix B.)

2. Then around the time scale $t \sim 1/\gamma_+$, the contribution from vacuum fluctuations of the field ($\langle \dots \rangle_v$) takes over so that Σ becomes quasi-steady and appears to settle down at a value depending on part of the initial data of the detectors. More explicitly, at this stage $q_+^{(\mu)}$, $\mu = A, B, +, -$ have been in their late-time values but $q_-^{(\mu)}$ are still about their initial values, so

$$\Sigma|_{t \sim 1/\gamma_+} \approx \frac{\hbar^4}{64} \left[\frac{\sin \Omega d}{\Omega d} e^{-2\gamma d} + 1 - \frac{2}{\hbar} \alpha^2 \Omega \right] \left[\frac{\sin \Omega d}{\Omega d} e^{-2\gamma d} + 1 - \frac{2\hbar}{\alpha^2 \Omega} + \frac{8\Lambda_1 \gamma}{\pi \Omega} \right] \quad (67)$$

in the weak-coupling and short distance approximation $\gamma \ll d\Omega^2 \ll \Omega$. Here Σ depends on α only; The parameter β in initial state (2) is always associated with $q_+^{(j)}$ in $\langle \dots \rangle_a$ so it becomes negligible at this stage (c.f. Eq.(25) in [1]). Note that $\Sigma|_{t \sim 1/\gamma_+}$ can be positive for small d only when α is at the neighborhood of $\sqrt{\hbar/\Omega}$.

3. The remaining initial data persist until a much longer time scale $t \sim 1/\gamma_-$ when Σ approaches a value consistent with the late-time results given in Sec. VI, which are contributed purely by the vacuum fluctuations of the field and independent of any initial data in the detectors. In this example the detectors have residual entanglement, though small compared to those in Stage 2.

The above behaviors in Stages 2 and 3 cannot be obtained by including only the first order correction from the mutual influences. Thus in this example we conclude that the mutual influences of the detectors at very short distance generate a transient entanglement between them in mid-session, while vacuum fluctuations of the field with the mutual influences included give the residual entanglement of the detectors at late times.

For the detectors initially entangled, only the early-time behavior looks different from the above descriptions. Their entanglement dynamics are similar to the above in the second and the third stages.

VIII. DISCUSSION

A. Physics represented by length scales

The physical behavior of the system we studied may be characterized by the following length scales:

Merge distance d_{min} in Eq.(20): Two detectors separated at a distance less than d_{min} would be viewed as those located at the same spatial point;

Radius of instability d_{ins} in Eq.(16): For any two detectors at a distance less than d_{ins} , their mode functions will grow exponentially in time so the quantum fluctuations of the detector diverge at late times;

Entanglement distance d_{ent} in Eq.(47): Two detectors at a distance less than d_{ent} will be entangled at late times, otherwise separable;

And d_0 defined in Sec. VC: for $d < d_0$ the zeroth order results breakdown. A stable theory should have d_{ent} and d_{min} greater than d_{ins} .

B. Direct interaction and effective interaction

In a closed bipartite system a direct interaction between the two parties, no matter how weak it is, will generate entanglement at late times. However, as we showed above, an effective interaction between the two detectors mediated by quantum fields will not generate residual entanglement (though creating transient entanglement is possible) if the two detectors are separated far enough, where the strength of the effective interactions is weak but not vanishing.

C. Comparison with 2HO QBM results

When $d \rightarrow d_{min}$ with large enough Ω , our model will reduce to a 2HO QBM model with real renormalized natural frequencies for the two harmonic oscillators. Paz and Roncaglia [15] have studied the entanglement dynamics of this 2HO QBM model and found that, at zero temperature, for both oscillators with the same natural frequency, there exists residual entanglement at late times in some cases and infinite sequences of sudden death and revival in other cases. In the latter case the averaged asymptotic value of negativity is still positive and so the detectors are “entangled on average”.

While our results show that the late time behavior of the detectors are independent of the initial state of the detectors, the asymptotic value of the negativity at late times in [15] does depend on the initial data in the detectors (their initial squeezing factor.) This is because in [15] the two oscillators are located exactly at the same point, namely, $d = 0$, so $\gamma_- = 0$ and the initial data carried by $q_-^{(j)}$ persists forever. Since in our cases d is not zero, the “late” time in [15] actually corresponds to the time interval with $(1/\gamma_+) \ll t \ll (1/\gamma_-)$ in our cases, which is not quite late for our detectors.

D. Where is the spatial dependence of entanglement coming from?

Two factors are responsible for the spatial dependence of entanglement. The first one is the phase difference of vacuum fluctuations that the two detectors experience. This is mainly responsible for the entanglement outside the light cone in all coupling strengths and those inside the light cone with sufficiently large separation in the weak-coupling limit, such as the cases in Sec.V. The second factor is the interference of retarded mutual influences, which are generated by back-reaction from the detectors to the field. It is important in the cases with small separation between the detectors, such as those in Sec.VII C.

E. Non-Markovian behavior and strong coupling

In our prior work [12] and [1], the non-Markovian behavior arises mainly from the vacuum fluctuations experienced by the detectors, and the essential temporal nonlocality in the autocorrelation of the field at zero temperature manifests fully in the strong-coupling regime. Nevertheless, in Sec. VII C one can see that, even in the weak-coupling limit, once the spatial separation is small enough and the evolution time is long enough, the mutual influences will create some non-Markovian behavior very different from those results obtained from perturbation theory with higher order mutual influences on the mode functions neglected.

Acknowledgement SYL wishes to thank Jen-Tsung Hsiang for helpful discussions. This work is supported in part by grants from the NSF Grants No. PHY-0426696, No. PHY-0601550, No. PHY-0801368 and the Laboratory for Physical Sciences.

APPENDIX A: LATE-TIME ANALYSIS ON MODE FUNCTIONS

Let

$$q_+^{(A)}(t) = \sum_j c_j e^{iK_j t}, \quad (\text{A1})$$

Eq.(12) gives

$$\sum_j c_j [-K_j^2 + 2i\gamma K_j + \Omega_r^2] e^{iK_j t} = \frac{2\gamma}{d} \sum_{j'} c_{j'} e^{iK_{j'}(t-d)}. \quad (\text{A2})$$

At late times, one is allowed to perform the Fourier transformation on both sides with t -integrations over $(-\infty, \infty)$ to obtain

$$-K_j^2 + 2i\gamma K_j + \Omega_r^2 = \frac{2\gamma}{d} e^{-iK_j d}. \quad (\text{A3})$$

There are infinitely many solutions for K_j in the complex K plane, so one needs infinitely many initial conditions to fix the factors c_j . Our q_+ chosen as a free oscillator at the initial moment and unaffected by its own history until

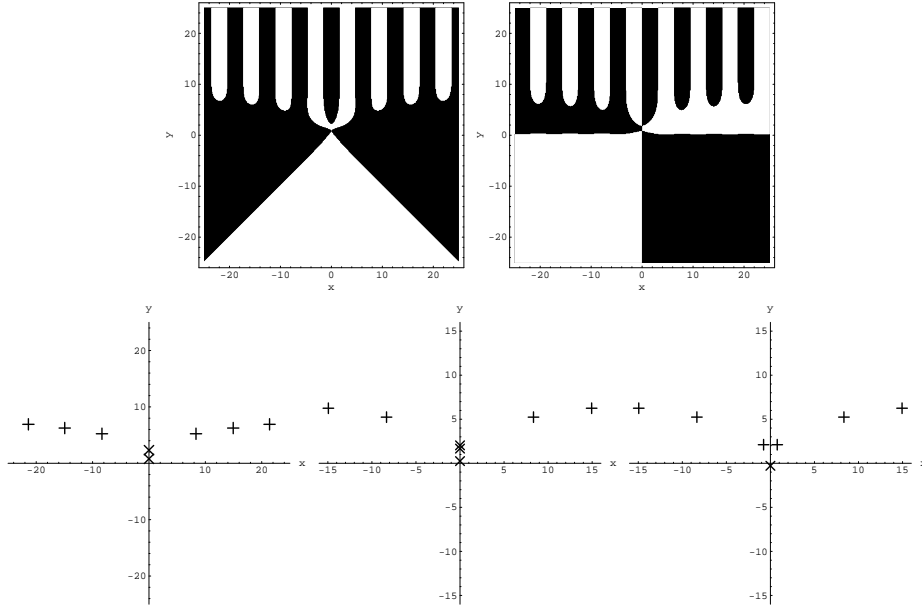


FIG. 6: The solutions to (A3) (or (A4) and (A5)) for the complex frequency $K_j = x_j + iy_j$ defined in (A1) are located at the intersections of the border lines in the upper plots. (Upper left) Left-hand-side (LHS) of (A4) is greater than right-hand-side (RHS) in the bright region, and less in the dark region. The border lines of the bright and the dark regions are solutions of (A4). Here $\gamma = 0.25$, $\Omega = 0.9000202$, $d = 1$. (Upper right) Similar for (A5). (Lower left) There are two purely imaginary solutions for K in this case. Here “+” denotes complex solutions and “x” denotes purely imaginary solutions. (Lower middle) Three purely imaginary solutions for K when $\gamma = 0.25$, $\Omega = 0.8$, $d = 1$. (Lower right) Solutions for K when $\gamma = 0.25$, $\Omega = 0.3$, $d = 1$. There is only one purely imaginary solution, which is located in the lower half of the complex K plane.

$t = d$ in principle can be specified by a set of c_j 's. Suppose this is true. Writing $K_j \equiv x_j + iy_j$, the real and imaginary parts of (A3) then read

$$(y - \gamma)^2 - x^2 + \Omega^2 = \frac{2\gamma}{d} e^{yd} \cos xd, \quad (\text{A4})$$

$$x(y - \gamma) = \frac{\gamma}{d} e^{yd} \sin xd. \quad (\text{A5})$$

The solutions for them are shown in Fig. 6. The left hand side of (A4) is a saddle surface over the xy space, while the right hand side of (A4) is exponentially growing in the $+y$ direction and oscillating in the x direction. For (A5), the situation is similar. From Fig. 6, one can see that there is no complex solution for K with nonvanishing real part and negative imaginary part ($x \neq 0$ and $y \leq 0$). The solutions for K with its imaginary part negative must be purely imaginary. Indeed, from (A5) and Fig. 6 (upper-right), one sees that when $x \neq 0$, if $y \leq 0$, then $(y - \gamma) \leq -\gamma$, but $-0.2172\gamma \lesssim \gamma e^{yd} (\sin xd)/(xd) < \gamma$, so there is no solution of (A5) with $y \leq 0$ and $x \neq 0$.

When $\Omega_r^2 > 2\gamma/d$, one finds that all solutions for K in (A3) are located in the upper half of the complex K plane, *i.e.*, all $y_j > 0$, which means that all modes in (A1) decay at late times.

When $\Omega_r^2 = 2\gamma/d$, there exists a solution $K = 0$, with other solutions on the upper half K plane. This implies that q_{R+} becomes a constant at late times.

When $\Omega_r^2 < 2\gamma/d$, there must exist one and only one solution for K with negative y , which corresponds to the unstable growing mode. This is consistent with our observation in Sec.IV.

Therefore, we conclude that $q_+^{(A)}$ is stable and decays at late times only for $\Omega_r^2 > 2\gamma/d$.

From (15) it seems that $q_-^{(A)}$ would oscillate at late times. However, similar analysis gives the conclusion that $q_-^{(A)}$ decays at late times for all cases. Thus, by symmetry, all $q_j^{(i)}$ decay at late times in the stable regime $\Omega_r^2 > 2\gamma/d$.

Now we turn to $q_{A,B}^{(+)}$. Eq.(7) implies that

$$\begin{aligned} (\partial_t^2 + 2\gamma\partial_t + \Omega_r^2)^2 q_B^{(+)}(t, \mathbf{k}) &= \left(\frac{2\gamma}{d}\right)^2 q_B^{(+)}(t - 2d, \mathbf{k}) + \\ &\lambda_0 e^{-i\omega t} \left[(-\omega^2 - 2\gamma\omega + \Omega_r^2) e^{ik_1 d/2} + \frac{2\gamma}{d} e^{i\omega d - ik_1 d/2} \right], \end{aligned} \quad (\text{A6})$$

at late times. Again, let

$$q_B^{(+)}(t, \mathbf{k}) = \sum_j c_{\mathbf{k}}^j e^{iK_{\mathbf{k}}^j t}, \quad (\text{A7})$$

then one has

$$\begin{aligned} \sum_j c_{\mathbf{k}}^j \left[-\left(K_{\mathbf{k}}^j\right)^2 + 2i\gamma K_{\mathbf{k}}^j + \Omega_r^2 \right]^2 e^{iK_{\mathbf{k}}^j t} &= \sum_j c_{\mathbf{k}}^j \left(\frac{2\gamma}{d}\right)^2 e^{iK_{\mathbf{k}}^j(t-2d)} + \\ &\lambda_0 e^{-i\omega t} \left[(-\omega^2 - 2i\gamma\omega + \Omega_r^2) e^{ik_1 d/2} + \frac{2\gamma}{d} e^{i\omega d - ik_1 d/2} \right]. \end{aligned} \quad (\text{A8})$$

After a Fourier transformation, for $K_{\mathbf{k}}^j \neq -\omega$, the above equation becomes

$$\left[-\left(K_{\mathbf{k}}^j\right)^2 + 2i\gamma K_{\mathbf{k}}^j + \Omega_r^2 \right]^2 = \left(\frac{2\gamma}{d}\right)^2 e^{-2iK_{\mathbf{k}}^j d}, \quad (\text{A9})$$

which is the squares of Eq.(A3) for $q_+^{(A)}$, or the counterpart for $q_-^{(A)}$. So these modes decay at late times for $\Omega_r^2 > 2\gamma/d$. On the other hand, if, say, $K_{\mathbf{k}}^0 = -\omega$, one has

$$\begin{aligned} [-\omega^2 + 2i\gamma\omega + \Omega_r^2]^2 c_{\mathbf{k}}^0 &= \left(\frac{2\gamma}{d}\right)^2 c_{\mathbf{k}}^0 e^{-2i\omega d} + \\ &\lambda_0 \left[(-\omega^2 - 2i\gamma\omega + \Omega_r^2) e^{ik_1 d/2} + \frac{2\gamma}{d} e^{i\omega d - ik_1 d/2} \right]. \end{aligned} \quad (\text{A10})$$

This equation will not hold unless

$$c_{\mathbf{k}}^0 = \frac{\lambda_0 \left[(-\omega^2 - 2i\gamma\omega + \Omega_r^2) e^{ik_1 d/2} + \frac{2\gamma}{d} e^{i\omega d - ik_1 d/2} \right]}{[-\omega^2 + 2i\gamma\omega + \Omega_r^2]^2 - \left(\frac{2\gamma}{d}\right)^2 e^{-2i\omega d}}. \quad (\text{A11})$$

Therefore, for $\Omega_r^2 > 2\gamma/d$, the only mode which survives at late times will be $e^{-i\omega t}$, and

$$q_B^{(+)}(t, \mathbf{k})|_{t \gg 1/\gamma} = c_{\mathbf{k}}^0 e^{-i\omega t}. \quad (\text{A12})$$

This is nothing but the sum of the $e^{-i\omega(t-nd)}$ part in Eq. (8) with $t \rightarrow \infty$ so summing from $n = 0$ to ∞ . Thus, (A12) with (A11) has included the mutual influences to all orders. The above analysis also indicates that the $e^{-\gamma(t-nd)}$ part in (8) really decays at late times for $\Omega_r^2 > 2\gamma/d$.

APPENDIX B: EARLY-TIME ANALYSIS IN WEAK-COUPPLING LIMIT

In the weak-coupling limit, the cross correlators $\langle \mathcal{R}_A, \mathcal{R}'_B \rangle$ with $\mathcal{R}, \mathcal{R}' = Q, P$ are small until one detector enters the other's lightcone. From this observation one could conclude that the cross correlations between the two detectors are mainly generated by the mutual influences sourced by the quantum state of the detectors and mediated by the field. This is not always true.

As shown in Sec.V A, the interference pattern has been there in the zeroth order results, where the mutual interferences on the mode functions are not included. Inserting the mode functions in the weak-coupling limit with the first order correction from the mutual influences into Eq.(25) in Ref. [1], when $t \ll O(1/\gamma\Lambda_i)$, $i = 0, 1$, the early-time Σ can be expressed as

$$\Sigma(t) \approx c_0 + b_0 t + a_0 t^2 + \theta(t-d) [b_1(t-d) + a_1(t-d)^2] + O(\gamma^3) \quad (\text{B1})$$

where c_0, b_j and a_j with $j = 0, 1$ depend on α, β and of $O(\gamma^0)$, $O(\gamma)$ and $O(\gamma^2)$, respectively. One can verify that the mutual influences are negligible in b_1 for the initial states with the value of β^2 not in the vicinity of \hbar^2/α^2 or $\alpha^2\Omega^2$. Indeed, a comparison of the upper plots in Fig. 7 and those in Fig. 1 shows that the corrections from mutual influences at early times are pretty small. Actually the early-time behaviors of Σ in both examples in Fig. 7 are

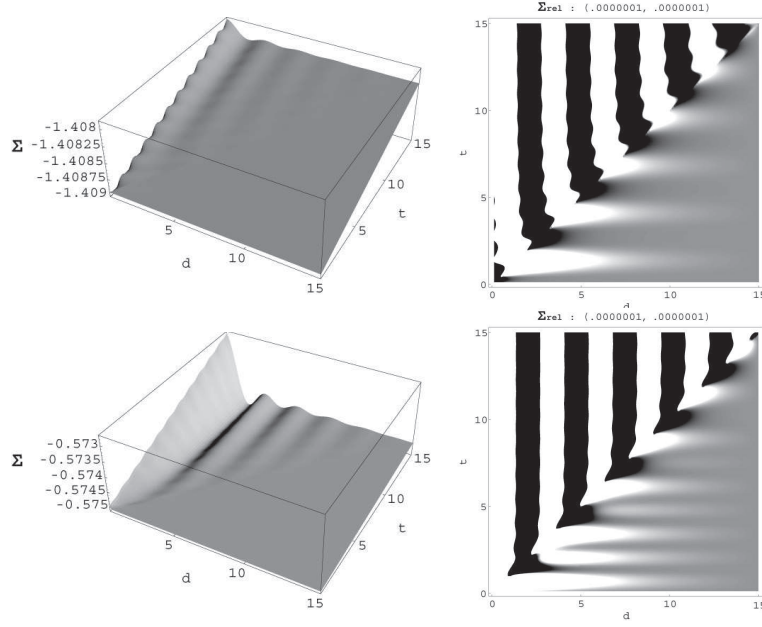


FIG. 7: The early-time evolution of Σ with the first order mutual influence included for different initial states of the detectors with $1/15 < d < 15$. (Upper row) All parameters are the same as those in Fig. 1 where $(\alpha, \beta) = (1.1, 4.5)$ and the initial state of the detectors is entangled. Compared with Fig. 1, one can see that the interference pattern is slightly distorted by the mutual influences. (Lower row) $(\alpha, \beta) = (1.5, 0.2)$, the detectors also initially entangled. The distortion by the mutual influences is tiny. As indicated by Eqs. (27) and (28), the complicated structure outside the lightcone is reducing to simple oscillations as time goes larger.

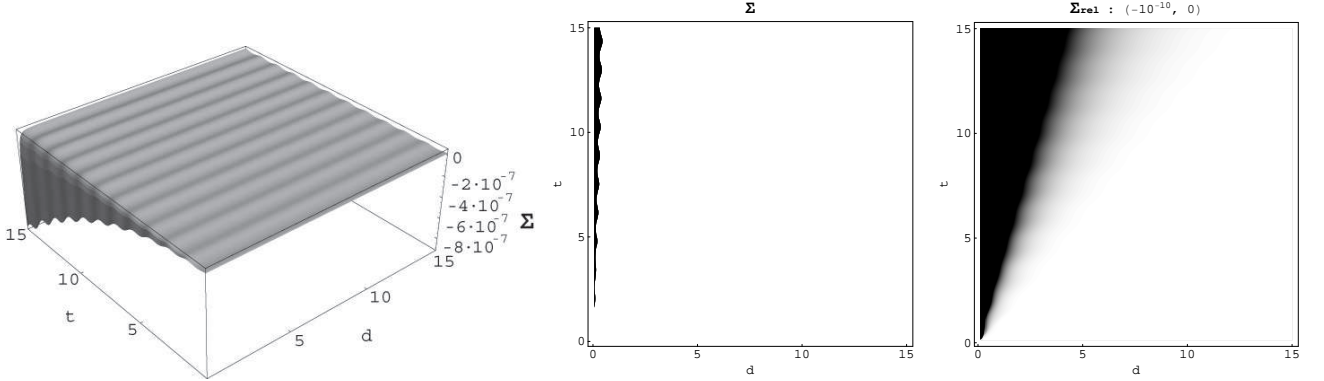


FIG. 8: The early-time evolution of Σ for an initially separable detector-pair with the first order mutual influence included. The parameters are the same as those in Fig. 1 except $(\alpha, \beta) = (1, 1)$ and $1/15 < d < 15$ here. From the left and middle plots, one finds that quantum entanglement is created at small d due to the mutual influences. (Σ is negative in the dark region of the middle plot.) For Σ_{rel} in the right plot, there is no clear interference pattern similar to those in Fig. 1, either inside or outside the lightcone. The detectors with smaller separation d always get a greater degree of entanglement.

dominated by the zeroth order results, thus by the phase difference of vacuum fluctuations in $\langle \mathcal{R}_A, \mathcal{R}_B \rangle_{\text{v}}^{(0)}$ rather than mutual influences [19].

In contrast, if the initial state (2) is separable ($\beta^2 \approx \hbar^2/\alpha^2$), the mutual influences will be important at early times. In this case, dropping all terms with small oscillations in time, one has

$$c_0 \approx \frac{\hbar^2}{4\pi^2\alpha^4\Omega^4} [\hbar^2\gamma\Lambda_1 + \alpha^4\Omega^2\gamma(2\Lambda_0 + \Lambda_1)]^2,$$

$$b_0 \approx \frac{\gamma\hbar^2}{2\pi\Omega^3} \left[2\Omega^2\gamma\Lambda_0 + \left(\frac{\hbar^2}{\alpha^4} + \Omega^2 \right) \gamma\Lambda_1 \right] (\hbar - \alpha^2\Omega)^2,$$

$$\begin{aligned}
a_0 &\approx \frac{\gamma^2 \hbar^2 (\hbar - \alpha^2 \Omega)^4}{4\Omega^2 \alpha^4}, \\
a_1 &\approx -\frac{\gamma^2 \hbar^2 (\hbar^2 - \alpha^4 \Omega^2)^2}{4\Omega^4 \alpha^4 d^2}.
\end{aligned} \tag{B2}$$

with b_1 negligible in (B1). The initial value of Σ is of the same order of c_0 , which is positive and determined by the numbers Λ_0 and Λ_1 corresponding to the cutoffs of this detector theory (the difference from the exact value is due to the oscillating terms dropped). For $\alpha^2 \neq \hbar/\Omega$ (Q_A and Q_B are each in a squeezed state initially), b_0 and a_0 are also positive definite, but a_1 is negative. When the separation d is sufficiently small, or

$$d < d_1 \equiv \frac{1}{\Omega} \left| \frac{\hbar + \alpha^2 \Omega}{\hbar - \alpha^2 \Omega} \right|. \tag{B3}$$

a_1 can overwhelm a_0 and alter the evolution of Σ from concave up to concave down in time. If this happens, the quantity Σ could become negative after a finite ‘‘entanglement time’’

$$t_{ent} \approx \frac{b_0 - 2a_1 d + \sqrt{(b_0 - 2a_1 d)^2 + 4|a_0 + a_1|(c_0 + a_1 d^2)}}{2|a_0 + a_1|}. \tag{B4}$$

This explains the plots in Fig. 8. The Σ_{rel} in the right plot is actually dominated by the a_1 term in (B1). (Note that such a prediction fails if $t_{ent} > O(1/\gamma\Lambda_i)$, $i = 0, 1$, and even for $t_{ent} < O(1/\gamma\Lambda_i)$ the above estimate on t_{ent} could have an error as large as $O(2\pi/\Omega)$ due to the dropped oscillating terms.) d_1 can serve as an estimate of the order for the maximum distance that transient entanglement can be generated. But note that for the detectors with the value of spatial separation between d_1 and d_{ent} the transient entanglement generated at early times will disappear at late times.

It is easy to verify that the first order correction of $\langle .. \rangle_a$ contribute the $a_1 \cos^2 \Omega d$ part of $a_1 = a_1(\cos^2 \Omega d + \sin^2 \Omega d)$, so with small enough separation d such that $\sin^2 \Omega d \ll \cos^2 \Omega d$ one can say that early-time entanglement creation is mainly due to the mutual influences of the detectors.

-
- [1] S.-Y. Lin, C.-H. Chou and B. L. Hu, Phys. Rev. D **78**, 125025 (2008) [arXiv: 0803.3995].
[2] T. Yu and J. H. Eberly, Phys. Rev. Lett. **93**, 140404 (2004).
[3] A. Einstein, B. Podolsky and N. Rosen, Phys. Rev. **47**, 777 (1935).
[4] C. Anastopoulos, S. Shresta and B. L. Hu, ‘‘Quantum Entanglement under Non-Markovian Dynamics of Two Qubits Interacting with a Common Electromagnetic Field’’, [quant-ph/0610007].
[5] J. D. Franson, J. Mod. Opt. **55**, 2117 (2008).
[6] Y. Aharonov, L. Vaidman, ‘‘Sending Signals to Space-Like Separated Regions’’, contribution to the ‘‘Mysteries and Paradoxes in Quantum Mechanics’’, Garda Lake 2000, [quant-ph/0102083].
[7] W. G. Unruh and R. M. Wald, Phys. Rev. D **52**, 2176 (1995).
[8] W. G. Unruh, ‘‘Is Quantum Mechanics Non-Local?’’ [quant-ph/9710032].
[9] Z. Ficek and R. Tanas, Phys. Rev. A **74**, 024304 (2006).
[10] K. Shiokawa, ‘‘Non-Markovian Dynamics and Entanglement in Quantum Brownian Motion’’, [arXiv: 0809.1587].
[11] S.-Y. Lin and B. L. Hu, Phys. Rev. D **73**, 124018 (2006) [gr-qc/0507054].
[12] S.-Y. Lin and B. L. Hu, Phys. Rev. D **76**, 064008 (2007) [gr-qc/0611062].
[13] R. Simon, Phys. Rev. Lett. **84**, 2726 (2000).
[14] C. H. Chou, T. Yu and B. L. Hu, Phys. Rev. E **77**, 011112 (2008).
[15] J. P. Paz and A. J. Roncaglia, Phys. Rev. Lett. **100**, 220401 (2008) [arXiv:0801.0464].
[16] C.-Y. Lai, J.-T. Hung, C.-Y. Mou and P. Chen, Phys. Rev. B **77**, 205419 (2008) [arXiv: 0803.0364].
[17] G. B. Arfken and H. J. Weber, *Mathematical Methods for Physicists* 6th Ed. (Elsevier, Amsterdam, 2005).
[18] Here we are talking about the entanglement dynamics of the system without measurements, the consideration of which is expected to bring forth consequences discussed in EPR [3]. In their classic paper the EPR gedanken experiment was introduced to bring out the incompleteness of quantum mechanics. The authors made no mention of ‘‘nonlocality’’. This notion crept in later for describing the situation when local measurements are performed at spacelike separations. Nonlocality does exist in e.g., noncommutative quantum field theory or in certain quantum theories of spacetime, but that is a much more severe breach of known physics, which need be dealt with at a more fundamental level than EPR entails.
[19] An interesting entanglement enhancement induced by the phase difference of vacuum fluctuations can be observed at $d \approx 2$ for $(\alpha, \beta) = (1.5, 0.2)$ in the lower plots of Fig. 7. The linear factor b_1 in (B1) is proportional to $\sin \Omega d / \Omega d$, whose minimum is about -0.2172 at $\Omega d \approx 4.4934$. This allows $b_0 + b_1$ for this initial state to be negative around $d \approx 4.4934/\Omega$. Accordingly the entanglement at early times is enhanced such that the disentanglement time for $d \approx 4.4934/\Omega$ is about two times longer than those for $d \approx 7.7253/\Omega$ (where the first peak of $\sin \Omega d / \Omega d$ is located).